Amyloid tracers binding sites in autosomal dominant and sporadic Alzheimer's disease

Ruiqing Ni[1], Per-Göran Gillberg[1], Nenad Bogdanovic[2, 6], Matti Viitanen[2, 4], Liisa Myllykangas[5], Inger Nennesmo[3], Bengt Långström[7], Agneta Nordberg[1, 4]

[1]Division of Translational Alzheimer Neurobiology; [2]Division of Clinical Geriatrics, Center for Alzheimer Research, Department of Neurobiology Care Sciences and Society, Karolinska Institutet, Stockholm, Sweden; [3]Division of Pathology, Department of Laboratory Medicine, [4]Department of Geriatric Medicine, Karolinska University Hospital Huddinge, Stockholm, Sweden; [5]Department of Pathology, University of Helsinki, Helsinki, Finland; [6]Department of Geriatric Medicine, University of Oslo, Oslo, Norway; [7]Department of Chemistry, Uppsala University, Uppsala, Sweden.

Published in Alzheimer's and Dementia, first published online 28 September 2016.

Doi: 10.1016/j.jalz.2016.08.006

Direct link to the final version of the article:

http://dx.doi.org/10.1016/j.jalz.2016.08.006

Title:

Amyloid tracers binding sites in autosomal dominant and sporadic Alzheimer's disease (84 characters)

Ruiqing Ni[1], Per-Göran Gillberg[1], Nenad Bogdanovic[2, 6], Matti Viitanen[2, 4], Liisa Myllykangas[5], Inger Nennesmo[3], Bengt Långström[7], Agneta Nordberg[1, 4]

[1]Division of Translational Alzheimer Neurobiology; [2]Division of Clinical Geriatrics, Center for Alzheimer Research, Department of Neurobiology Care Sciences and Society, Karolinska Institutet, Stockholm, Sweden; [3]Division of Pathology, Department of Laboratory Medicine, [4]Department of Geriatric Medicine, Karolinska University Hospital Huddinge, Stockholm, Sweden; [5]Department of Pathology, University of Helsinki, Helsinki, Finland; [6]Department of Geriatric Medicine, University of Oslo, Oslo, Norway; [7]Department of Chemistry, Uppsala University, Uppsala, Sweden.

Title: 84 characters (limit 85 characters)
Number of words in abstract: 150 words (limit 150 words)
Number of figures: 6
Number of tables: 2
Number of words in the manuscript: 3441 words (limit 3500 words)
Number of References: limit 50
Number of words in Research in Context: 159 words (limit 150 words)

Corresponding author: Agneta Nordberg, MD, PhD, Professor,
Karolinska Institutet, Department of Neurobiology, Care Sciences and Societies, Center for Alzheimer research, Division of Translational Alzheimer Neurobiology, Novum 5th Floor, Blickagången 6, S-141 57 Stockholm, Sweden.
Telephone: +46 8 585 85467
Fax: +46 8 585 85470
E-mail: Agneta.K.Nordberg@ki.se

Abstract

INTRODUCTION: Amyloid imaging has been intergrated into diagnostic criteria for Alzheimer´s disease (AD). How amyloid tracers binding differ for different tracer structure and amyloid-β aggregate in autosomal dominant AD (ADAD) and sporadic AD is unclear.

METHODS: Binding properties of different amyloid tracers were examined in brain homogenates from six ADAD with *APPswe*, *PS1M146V* and *PS1EΔ9* mutations, thirteen sporadic AD and fourteen control cases.

RESULTS: ^{3}H-PIB, ^{3}H-florbetaben, ^{3}H-AZD2184 and BTA-1 shared a high- and a varying low-affinity binding site in the frontal cortex of sporadic AD. AZD2184 detected another binding site (affinity 33 nM) in the frontal cortex of ADAD. The ^{3}H-AZD2184 and ^{3}H-PIB binding were significantly higher in the striatum of ADAD compared to sporadic AD and control. Polyphenol resveratrol showed strongest inhibition on ^{3}H-AZD84 binding followed by ^{3}H-florbetaben and minimal on ^{3}H-PIB.

DISCUSSION: This study implies amyloid tracers of different structures detect different sites on amyloid-β fibrils or conformations.

Keywords: Alzheimer's disease; amyloid-β; Autosomal dominant Alzheimer's disease; Positron emission tomography; Resveratrol; Pittsburgh compound B; AZD2184; Florbetaben

1. Introduction

The rapid development of molecular imaging enables measurement of brain amyloid-β (Aβ) plaques *in vivo* and facilitates an early detection of AD [1]. From the initial amyoid PET studies with ^{11}C-Pittsburgh compound B (PIB), three PET tracers ^{18}F-florbetapir, ^{18}F-florbetaben and ^{18}F-flutemetamol have been approved by US Food and Drug Administration and European Medical Assocation for use in clinical assessement of memory impairment to exclude AD.

Subjects clinically diagnosed with AD without Aβ plaques at autopsy or PIB PET negative AD patients included in Aβ immunization trials [2] raise the questions of clinical variants of AD or misdiagnosis of AD. Appropriate use of biomarkers such as Aβ PET will improve diagnostic accuracy. Aβ tracers might vary in their binding properties to different Aβ fibrils and thereby provide new insight into pathophysiological mechanisms and variants of AD. In silico modelling studies have suggested six different surface and core binding sites on synthetic Aβ fibrils similarly using thioflavine-T compound (e.g. PIB), florbetaben and florbetapir [3-5]. Three binding sites have been demonstrated on synthetic Aβ fibrils [6]. A multiple-binding site model for Aβ tracers was suggested in AD autopsy brain where florbetapir, florbetaben and PIB mainly bind to a high-affinity site 1 (nanomolar range), BF-227 mainly with low-affinity to site 3 and FDDNP partly binding to site 2 [7].

Autosomal dominant AD (ADAD) [8] characterized by atypical forms of Aβ aggregates represents interesting models to study target engagement of Aβ tracer to fibrillar as well as other Aβ conformations. Prominent ^{11}C-PIB retentions have been reported in ADAD carrying *PS1*, *APP* mutation, in cortical and particularly subcortical brain regions [9-15]. In two exceptions *APParc* [13] and *APPEΔ693* [16], low cortical ^{11}C-PIB retention was reported compared to sporadic AD (sAD) probably due to ring-shaped plaques or oligomeric Aβ accumulation in the brain.

In the present study we compared the binding characteristic of Aβ PET tracers ^{3}H-PIB, ^{3}H-AZD2184, ^{3}H-florbetaben, and methyl-^{3}H-BTA-1 in autopsy brain tissue from the frontal cortex and striatum of patients with sAD and ADAD respectively. An additional third binding site was detected by AZD2184 in the frontal cortex of ADAD patients as opposite to the other Aβ tracers. High AZD2184 and PIB binding was measured in the striatum of ADAD compared to sAD. In addition, AZD2184 competed in nanomolar range with anti-Aβ phenol compound resveratrol. The Aβ binding properties

seem to depend both on the chemical structures of Aβ tracers as well as the conformation of Aβ aggregates.

2. Methods

2.1 Materials:

[^{3}H]-2-[6-(methylamino)pyridin-3-yl]-1,3-benzothiazol-6-ol (^{3}H-AZD2184, specific activity (SA) 21.9 Ci/mmol) and AZD2184 were synthesized at the Karolinska Institutet PET Radiochemistry Laboratory, Stockholm, Sweden. [N-*methyl*-^{3}H]2-(4'-methylaminophenyl)-6-hydroxybenzothiazole (^{3}H-PIB, SA 85 Ci/mmol) and Methyl-^{3}H-BTA-1, (SA 84 Ci/mmol) were synthesized by Quotient Bioresearch, Cardiff, UK. [N-*methyl*-^{3}H]4-[(E)-2-(4-{2-[2-(2-fluoroethoxy)ethyl]ethoxy}phenyl) ethenyl]-aniline (^{3}H-florbetaben, SA 63 Ci/mmol) and florbetaben were synthesized by Bayer Healthcare Pharmaceuticals, Berlin, Germany. 2-(4´-Methylaminophenyl)benzothiazole (BTA-1), 4,5-trihydroxy-trans-stilbene (resveratrol) were purchased from Sigma Aldrich, MO, USA. **Fig. 6** showed the chemical structures of amyloid tracers and resveratrol drawn using ChemDraw Standard 14.0 (CambridgeSoft, Perkin Elmer, MA, U.S.A.).

2.2 Sporadic AD, ADAD and control brain studies

Frontal cortex and striatum (caudate nucleus and putamen) tissues from 13 patients with sAD (mean age 68.2 ± 8.5 y), clinically diagnosed and confirmed by pathological examination according to NINCDS-ADRDA criteria and 14 age-matched controls (mean age 74.1 ± 12.0 y) were obtained at autopsy and provided by the Netherlands Brain Bank, Netherlands Institute for Brain Research, Amsterdam, Netherland (**Table 1**). Brain tissue from six ADAD cases including three *APPswe* mutation carriers (mean age 63.3 ± 3.7 y), one *PS1 M146V* mutation carriers (age 48 y), were provided by the Brain Bank at Karolinska Institutet, Stockholm, Sweden. Brain tissue from one *PS1 M146V* mutation carrier (age 43 y), and one *PS1 EΔ9* mutation carrier (age 66 y) were provided from the Department of Pathology, University of Helsinki, Helsinki, Finland. Permission to use autopsy brain material in experimental procedures was granted by the Regional Human Ethics committee in Stockholm and the Swedish Ministry of Health, and Ethics Committee of the Northern Ostrobothnia

Hospital District, Finland. Brain regions were dissected following recommendation of BrainNet Europe for fixation and anatomical dissection (www.brainnet-europe.org).

2.3 Bielschowsky silver staining in ADAD and sporadic Alzheimer's cases

For neuropathological investigations, brain tissues from ADAD and sAD were fixed in buffered 4 % formaldehyde for 4-6 weeks, paraffinized and cut to 5 μm thick sections from the frontal medial gyrus and striatum. The sections were stained in the same laboratory condition by Bielschowsky silver impregnation according Yamamoto modification [17].

2.4 Saturation assays in the frontal cortex homogenates from sporadic AD

Post-mortem frontal cortex brain tissue homogenates (100 μg tissue) from patients with sAD were incubated with 0.01-250 nM ^{3}H-AZD2184, ^{3}H-PIB, ^{3}H-florbetaben and methyl-^{3}H-BTA-1 in 1 x PBS buffer (pH 7.4) for 2 hr at room temperature. Non-specific binding was determined in the presence of 1 μM BTA-1. Samples were run in triplicates and the specific binding was expressed in pmol/g tissue. The dissociation constant (K_d) and maximum number of binding sites (B_{max}) was determined using non-linear regression models in GraphPad Prism version 6.0 (GraphPad Software, Inc., La Jolla, CA, USA). The saturation data were fit to one-site and two-site binding model, followed by F-test for model selection. Scatchard plots were obtained using GraphPad Prism to display the saturation data.

2.5 Competitive binding studies in frontal cortical and striatum homogenates from sporadic AD and ADAD

Competitive binding assays comparing different amyloid tracers in sAD frontal cortex brains were carried out by incubating homogenates (100 μg tissue) with 1.0 nM ^{3}H-PIB, 2.5 nM ^{3}H-florbetaben, 1.5 nM ^{3}H-AZD2184 or 2.0 nM methyl-^{3}H-BTA-1 in the presence of unlabeled AZD2184, BTA-1, florbetaben and at concentrations ranging from 10^{-11}-10^{-4} M. Competition binding assays comparing ^{3}H-PIB binding properties in sAD and ADAD (*APPswe*, *PS1 M146V* and *PS1 EΔ9*) brain, were carried out by incubating frontal cortex and striatum homogenates (100 μg tissue) with 1.0 nM ^{3}H-PIB in the presence of BTA-1 and AZD2184 at concentrations ranging from 10^{-11}-10^{-4} M. The

affinity constant (K_i) and percentage of displacement were determined by using non-linear regression one-site and two-site binding models derived from Cheng-Prusoff equation in GraphPad Prism, followed by F-test for model selection. The three-site binding of ^{3}H-PIB/AZD2184 competitive binding in the frontal cortex from ADAD were analyzed by additional fitting using two-site binding model in GraphPad Prism with binding data at AZD2184 concentration ranging from 10^{-9} to 10^{-4} M.

2.6 Regional ^{3}H-PIB and ^{3}H-AZD2184 binding in brain tissue homogenates from sporadic AD, ADAD and healthy controls

Single concentration binding studies using 1.0 nM ^{3}H-PIB, and 1.5 nM ^{3}H-AZD2184 were carried out by incubating homogenates (200 μg tissue) from the frontal cortex and striatum of sAD and ADAD (*APPswe*, *PS1 M146V, PS1 EΔ9* mutation carriers) and control brains. Non-specific binding was determined in the presence of 1 μM BTA-1.

2.7 Interaction of resveratrol on amyloid tracer binding in the frontal cortical homogenates from patients with sporadic AD

To determine the influence of phenols on amyloid tracer binding, frontal cortex homogenates from three sAD were incubated with 1.5 nM ^{3}H-AZD2184, 2.5 nM ^{3}H-florbetaben and 1.0 nM ^{3}H-PIB in the presence of resveratrol at concentrations of 10^{-11}-10^{-4} M.

2.8 Statistical analysis

Data were analyzed using GraphPad Prism version 6.0. Nonparametric Mann-Whitney test was used for comparisons between groups. All values are shown as means ± standard deviation (SD). Error bars in the figures represent standard error (S.E.M) values. Significant differences between groups were set at *$p < 0.05$, **$p < 0.01$, ***$p < 0.001$.

3. Results

3.1 Bielschowsky silver staining in sporadic AD and ADAD

When Bielschowsky silver staining was performed in brain sections of *APPswe*, *PS1 M146V* and *PS1 EΔ9* cases. ADAD showed a more intensive neuritic plaque staining in the layer I-III of frontal medial gyrus compared to sporadic AD cases **(Fig. 1 A-D**). The largest plaques were observed in the cortex of *PS1 EΔ9* case reaching the size of 100 μm in diameter. In *PS1 M146V* cases, neurofibrillry tangles and treads that were less present, with the feature of heavy loaded silver impregnated neuritic plaques indicating the presence of additional fibrillary pathology in the plaques. *APPswe* and *PS1 M146V* cases showed intensive silver impregnation in the striatum; while for *PS1 EΔ9* cases as well as sporadic AD cases, there was an abundance of plaques in the striatum although the silver staining was weaker indicating their more diffuse nature **(Fig. 1 E-H).**

3.2 Comparison of the binding properties of different amyloid tracers in the frontal cortex and striatum of sporadic AD and ADAD

In order to characterize the binding sites of the amyloid tracers ^{3}H-AZD2184, ^{3}H-PIB, ^{3}H-florbetaben and methyl-^{3}H-BTA-1, saturation-binding studies using increasing concentrations (0.01 - 250 nM) of these tracers were performed in the frontal cortex homogenates from sAD patients**. Fig. 2** illustrates the saturation curves and Scatchard plots. Two binding sites could be obtained for ^{3}H-AZD2184 (K_d: 6.5 nM, 50.4 nM), ^{3}H-PIB (K_d: 2.5 nM, 81.7 nM) and ^{3}H-florbetaben (K_d: 9.7 nM, 135 nM) respectively. Comparable binding affinity (K_d) for the high-and low-affinity binding sites, and B_{max} for the high-affinity site were obtained for three amyloid tracers. No definite binding sites could be detected with the tracer methyl-^{3}H-BTA-1 due to high percentage of non-specific binding.

To further characterize and compare the binding properties of the amyloid tracer, competition studies were performed in the frontal cortex homogenates from sAD cases with ^{3}H-AZD2184, ^{3}H-PIB, ^{3}H-florbetaben and methyl-^{3}H-BTA-1 in the presence of increasing concentration of unlabeled BTA-1, AZD2184 and florbetaben (10^{-11}-10^{-4} M) respectively. Analysis of the competition results demonstrated the presence of a similar high-affinity site and varying low-affinity sites of ^{3}H-AZD2184, ^{3}H-PIB and ^{3}H-florbetaben in sAD frontal cortex (**Fig. 3).**

^{3}H-PIB showed two binding sites for unlabeled AZD2184 (K_i: 0.1 nM, 125 nM), BTA-1 (K_i: 0.9 nM, 83 nM), and florbetaben (K_i: 0.1 nM, 190 nM) in the sAD frontal cortex. ^{3}H-AZD2184 demonstrated a wide range of low-affinity binding sites with unlabeled AZD2184 (K_i: 0.1 nM, 7 nM), BTA-1 (K_i:

0.1 nM, 53 nM), and florbetaben (K_i: 0.2 nM, 325 nM). For ^{3}H-florbetaben, two sites with comparable affinities were obtained with AZD2184 (K_i: 0.5 nM, 24 nM), BTA-1 (K_i: 0.1 nM, 45 nM) and florbetaben (K_i: 0.1 nM, 32 nM) respectively. Methyl-^{3}H-BTA-1 binding contained high percentage of non-specific component and one binding site was estimated for florbetaben ($\approx$ 20 nM), AZD2184 ($\approx$ 200 nM) and BTA-1 ($\approx$ 1000 nM) (**Fig. 3**).

To investigate the difference between amyloid binding sites in ADAD and sAD brain, ^{3}H-PIB competitive binding assays were performed using unlabeled AZD2184 or BTA-1 in the frontal cortex and striatum from six ADAD patients (including three *APPswe,* two *PS1 M146V* and one *PS1 EΔ9* mutation carriers). In the frontal cortex from ADAD, three binding sites were demonstrated using AZD2184 (K_i: 0.5 nM, 33 nM, 327 nM), while two binding sites with unlabelled BTA-1 (K_i: 1.3 nM, 80 nM) (**Fig. 4 A**). In the striatum of ADAD, two binding sites were detected using AZD2184 (K_i: 0.6 nM, 95 nM) and BTA-1 (K_i: 0.8 nM, 37 nM). The ^{3}H-PIB/BTA-1 binding affinity was somewhat higher in the striatum of ADAD cases compared to that of sAD (K_i: 4.8 nM, 105 nM) (**Fig. 4B**).

3.3 Regional amyloid tracer binding in autosomal dominant and sporadic Alzheimer's disease

The binding of a single concentration of ^{3}H-PIB (1.0 nM) and ^{3}H-AZD2184 (1.5 nM) was measured in the homogenates from frontal cortex and striatum of six ADAD cases (including three *APPswe*, two *PS1 M146V*, one *PS1 EΔ9* mutation carriers), thirteen sAD cases, and fourteen controls respectively. Although the three ADAD mutations showed different properties of plaque pathology (**Fig. 1 A-H**) the ADAD cases were analysed together due to few cases from each mutation. A significant higher number of ^{3}H-PIB and ^{3}H-AZD2184 binding sites were observed in the frontal cortex of both ADAD and sAD cases compared to healthy controls **(Table 2).** A significant higher ^{3}H-PIB as well as the ^{3}H-AZD2184 binding was measured in the striatum of ADAD cases compared to control cases while no significant difference in binding was observed between sAD and controls (**Table 2**). Of the DAD cases both cases with APPswe and the PSM146V encoded mutations showed heavy plaque load in the striatum (**Fig. 1 E-H**).

3.4 Interaction of resveratrol with amyloid tracers binding in the frontal cortex of sporadic Alzheimer's disease

To investigate the possible interactive mechanisms between resveratrol and Aβ tracers binding sites in sAD brain, competitive binding assays were performed using resveratrol (10^{-11}-10^{-4} M) and ^{3}H-AZD2184 (1.5 nM), ^{3}H-PIB (1.0 nM), ^{3}H-florbetaben (2.0 nM) respectively in homogenates prepared from the frontal cortex of three sAD cases. Analysis of the resveratrol competition binding studies demonstrated an interaction with a high-affinity binding site for ^{3}H-AZD2184 ($K_i \approx$ 5 nM), while for ^{3}H-florbetaben to a low affinity site ($K_i \approx$ 238 nM) and a very low affinity site for ^{3}H-PIB ($K_i \approx$ 1900 nM) **(Fig 5).**

4. Discussion

Amyloid PET imaging has advanced our understanding of the early pre-symptomatic deposition of fibrillar Aβ in patients with ADAD and sAD [14, 18, 19]. There is a need to understand the interaction of Aβ ligands on the different binding sites on the Aβ fibril β-sheet and to clarify their biological role and possible technical confounders [20-22]. In this study, we examined the *in vitro* properties of Aβ tracers and studied how different chemical structures (**Fig. 6**) could influence the interaction of different Aβ conformation characteristics in ADAD and sAD cortical and striatal brain tissue, providing a link between binding and Aβ neuropathology.

Clinical studies using different Aβ PET tracers have shown comparable results in detecting the presence of fibrillar Aβ plaques in brain from sAD and mild cognitive impairment using ^{11}C-PIB [23], ^{18}F-florbetaben [24], ^{18}F-florbetapir, ^{18}F-flutemetamol [25, 26], ^{18}F-NAV4694 [27]. Head to head comparison of ^{11}C-PIB and ^{18}F-AZD4694 have shown strong correlation in binding [27] as well as between the three tracers ^{11}C-PIB, ^{18}F-florbetapir and ^{18}F-flutemetamol [28]. In Aβ microPET in transgenic AD rat brain, excessive NAV4694 (an AZD2184 analog) blocked only 10-25 % ^{11}C-PIB binding, suggesting that these two tracers may bind to different sites or forms of Aβ [29]. Such competitive experiment is highly informative, but not available in AD patients.

^{3}H-PIB binding correlates with amyloid plaques loads in sAD brain [30, 31], including neuritic plaques, cerebral angiopathy (CAA), diffuse plaques but not amorphous amyloid plaques in AD brain [32]. ^{18}F-flutemetamol [26], ^{18}F-florbetapir [33] and ^{18}F-florbetaben PET has shown high sensitivity and specificity for the detection of histopathology-confirmed neuritic Aβ plaques. A subfraction of Aβ has been found containing high-affinity ^{3}H-PIB site in sAD brain [34]. Recent

studies reported that Thal phase but not CERAD score correlate with PIB SUV from antemortem imaging , and suggesting that diffuse plaques may contribute to the PIB signal in PET imaging [32].

From the chemical structure perspective, Thioflavine T derived tracer ^{3}H-AZD2184, ^{3}H-PIB, methyl-^{3}H-BTA-1 and stilbene derived tracer ^{3}H-florbetaben all share a planar structure. In addition, florbetaben contains a more flexible polyethylene glycol (PEG) chain, which maintain lipophilicity and neutrality may influence the compounds engagement with β-sheet structure [35]. All studied Aβ tracers (^{3}H-florbetaben, ^{3}H-AZD2184, ^{3}H-PIB) except ^{3}H-Me-BTA-1, showed both a high- and low-affinity binding sites in AD brain tissue, in agreement with earlier studies [7]. AZD2184 showed higher affinity of binding sites in the frontal cortex of sAD as well as a third binding site in the frontal cortex of ADAD, supporting multiple binding site model on fibrillar Aβ in brain. Earlier biophysical modeling studies have identified six possible binding sites for Aβ tracers PIB, BTA-1 and Thioflavine T [3, 4]. Florbetaben, florbetapir and PIB that of different scaffolds share a common binding mode to surface groove, while the particular binding position and affinity might vary between different amyloid tracer and morphology of Aβ fibril [5] which is in line with present study. When the binding profile of AZD2184 and thioflavine was studied by molecular docking and molecular dynamic simulation four binding sites were observed on the Aβ fibril where three with the fibril and one on the two sides of the Met35 residue on the surface [35]. The binding affinity of AZD2184 was found to be higher than thioflavine due to electrostatic interaction and spatial restriction [35]. Additionally, factors such as lipophilicity, pKa and the overall tracer structure may influence the tracer binding properties and the low non-specific binding of ^{3}H-AZD2184 has been attributed partly to its low lipophilicity (^{3}H-AZD2184 < ^{3}H-PIB < ^{3}H-florbetaben < Methyl-^{3}H-BTA-1) [36, 37].

We found that resveratrol interacted with the rank of order AZD2184 > florbetaben > PIB. Several possible mechanisms have been proposed regarding resveratrol-Aβ interaction, including specific conformation or non-covalent interaction with β-sheet structure [38] or with Aβ sequence such as the $A\beta_{17-21}$ aromatic phenylalanine residue . Resveratrol are currently under clinical trial and phase II clinical trial in AD patients (NCT01504854). Interestingly enough resveratrol is phenol with stilbene structure. Resveratrol has been shown to inhibit synthetic Aβ aggregation and toxicity *in vitro* [39], and detected fluorescence of Aβ plaques similarly as Thioflavin T in post-mortem AD brain slides [40, 41]. The indication of direct binding of resveratrol to Aβ has raised an interest in developing resveratrol derivatives as potential Aβ PET tracers [42] and luminescent conjugated polymers as well as AD treatment agent. In a recent study administration of resveratrol (200 mg/day) for 26 weeks in

healthy, overweight older adult showed an improvement in memory performance as well as improved glucose metabolism [43].

Recent Alzheimer Disease Neuroimaging Initiative (ADNI) study and Dominantly Inherited Alzheimer Network (DIAN) has identified higher total Aβ load and less varitiety in comorbidity in ADAD brain [44]. We examined the properties of different Aβ tracers in brain tissue from mutation carriers with different characteristic AD pathology [45-49] and compared with that in sAD. We demonstrated that the number of striatal ^{3}H-PIB and ^{3}H-AZD2184 binding sites in ADAD was higher compared to sAD, and did not differ in the frontal cortex between two AD groups. This observation is in agreement with an earlier report [10], which also demonstrated a higher ^{11}C-PIB retention *in vivo* in the striatum of *PS1 EΔ9* AD patients compared to sAD. The lower intensity of silver impregnation of the plaques (mainly diffuse) in the striatum of *PS1 EΔ9* mutation case underline the unique biochemical feature of the fibrillation of that mutation. *PS1 EΔ9* mutation carriers are known for their characteristic pathology of "cotton wool" plaques and CAA in the frontal cortex and widespread small diffuse Aβ plaques devoid of dystrophic neurites in the striatum [48]. The finding suggests that Aβ tracers can detect diffuse plaques. The arctic APP mutation carriers are lacking the β-sheet formation and show low ^{11}C-PIB brain retention [13]. A very high plaque load is presented in the *APPswe* and *PS1 M146V* brain tissue. Despite that Aβ tracers have been suggested to bind to late fibrillar forms, the findings in the present study suggest that intensity of the binding thus not only depends on the morphological feature of the silver impregnation but probably rather more to specific biochemical properties of the plaques especially in the particular mutation the sensitivity of the ligand binding even to the mutation-specific earlier/diffuse plaque.

There are some limitations of this study. Firstly, the fact that the availably of autopsy brain material is rare from these very unusual mutations which do not allowing large-scale studies. Secondly, i*n vitro* solid-state nuclear magnetic resonance studies suggest that the molecular structures of Aβ fibrils vary in different sAD brains, which may contribute to the observed variation [50]. For quality control of the present study, the experiments were therefore repeated independently more than time and the binding curve analysis were evaluated independently and discussed between three of the authors. Thirdly, the variance in the competitive binding studies with resveratrol and different amyloid tracer were rather large as resveratrol is not specific for Aβ fibrils.

Understanding the binding mode of different amyloid tracers to brain Aß aggregates may facilitates the development of new early biomarkers as well as designing new drug targets for AD therapies. Future study regarding the pathological properties of the arctic and E293 Δ mutations brains including studies of regional tau deposition and astrocytes activation will be insightful. New strategies for developing new Aß tracers that can detect smaller forms of Aß oligomeric forms as well protofibril are of great interest and should be tested in in silico modeling as well as in ADAD especially arctic mutation brain tissue and further also be explored by in vivo imaging in ADAD subjects at risk as well as sAD patients . Competitive binding using different amyloid compound *in vivo* in AD patients would be informative for but might be difficult due to the high concentrations needed of the tracers. In addition, it will be of clinical relevance to study how differences in properties of amyloid tracers could discriminate between rapidly progressive AD compared to slowly progressive AD cases and also might detect variants of late-onset sAD with divergent Aß pathology.

To conclude, the studied Aβ tracers in the present study showed multiple binding sites and different binding properties in ADAD in comparison to sAD brains. AZD2184 detected, a third Aβ binding sites in the ADAD frontal cortex. High binding of the Aβ tracers in ADAD striatal tissue suggests conformal differences of amyloid aggregates in ADAD compared to sAD, confirming earlier *in vivo* PET observations in the cortex and striatum of sAD and ADAD patients. The anti-amyloid phenol compound resveratrol interacted in Nano molar range with AZD2184 but showed less affinity for florbetaben followed by PIB. Studies of the target similarity, differences as well as selectivity properties between the different amyloid tracers and *in vivo*-postmortem validation will facilitate the development of new imaging and therapeutic agents action on specific Aß conformational aggregates.

Funding

This work was supported by grants from the Swedish Research Council (project 05817), Swedish Foundation for Strategic Research (SSF), Karolinska Institutet Strategic Neuroscience program, the Stockholm County Council-Karolinska Institutet regional agreement on medical training and clinical research (ALF grant), Swedish Brain Power, the Swedish Brain Foundation, the Alzheimer Foundation in Sweden, European Union's Seventh Framework Programme (FP7/2007-2013) under

grant agreement n° HEALTH-F2-2011-278850 (INMiND), the Foundation for Old Servants, Karolinska Institutet’s Foundation for Aging Research, Gun and Bertil Stohne's Foundation, Sigurd and Elsa Golje's Foundation, Ragnhild and Einar Lundström's Memorial Foundation, Demensfonden.

References:

[1] Dubois B, Feldman HH, Jacova C, Hampel H, Molinuevo JL, Blennow K, et al. Advancing research diagnostic criteria for Alzheimer's disease: the IWG-2 criteria. Lancet Neurol. 2014;13:614-29.
[2] Liu E, Schmidt ME, Margolin R, Sperling R, Koeppe R, Mason NS, et al. Amyloid-beta 11C-PiB-PET imaging results from 2 randomized bapineuzumab phase 3 AD trials. Neurology. 2015;85:692-700.
[3] Wu C, Bowers Michael T, Shea J-E. On the Origin of the Stronger Binding of PIB over Thioflavin T to Protofibrils of the Alzheimer Amyloid-β Peptide: A Molecular Dynamics Study. Biophysical Journal. 2011;100:1316-24.
[4] Murugan NA, Olsen JMH, Kongsted J, Rinkevicius Z, Aidas K, Ågren H. Amyloid Fibril-Induced Structural and Spectral Modifications in the Thioflavin-T Optical Probe. The Journal of Physical Chemistry Letters. 2012;4:70-7.
[5] Skeby KK, Sørensen J, Schiøtt B. Identification of a Common Binding Mode for Imaging Agents to Amyloid Fibrils from Molecular Dynamics Simulations. Journal of the American Chemical Society. 2013;135:15114-28.
[6] Ye L, Morgenstern JL, Gee AD, Hong G, Brown J, Lockhart A. Delineation of Positron Emission Tomography Imaging Agent Binding Sites on β-Amyloid Peptide Fibrils. Journal of Biological Chemistry. 2005;280:23599-604.
[7] Ni R, Gillberg PG, Bergfors A, Marutle A, Nordberg A. Amyloid tracers detect multiple binding sites in Alzheimer's disease brain tissue. Brain. 2013;136:2217-27.
[8] Bettens K, Sleegers K, Van Broeckhoven C. Genetic insights in Alzheimer's disease. Lancet Neurol. 2013;12:92-104.
[9] Klunk WE, Price JC, Mathis CA, Tsopelas ND, Lopresti BJ, Ziolko SK, et al. Amyloid deposition begins in the striatum of presenilin-1 mutation carriers from two unrelated pedigrees. J Neurosci. 2007;27:6174-84.
[10] Koivunen J, Verkkoniemi A, Aalto S, Paetau A, Ahonen JP, Viitanen M, et al. PET amyloid ligand [11C]PIB uptake shows predominantly striatal increase in variant Alzheimer's disease. Brain. 2008;131:1845-53.
[11] Villemagne VL, Ataka S, Mizuno T, Brooks WS, Wada Y, Kondo M, et al. High striatal amyloid beta-peptide deposition across different autosomal Alzheimer disease mutation types. Arch Neurol. 2009;66:1537-44.
[12] Knight WD, Okello AA, Ryan NS, Turkheimer FE, Rodriguez Martinez de Llano S, Edison P, et al. Carbon-11-Pittsburgh compound B positron emission tomography imaging of amyloid deposition in presenilin 1 mutation carriers. Brain. 2010;134:293-300.
[13] Scholl M, Wall A, Thordardottir S, Ferreira D, Bogdanovic N, Langstrom B, et al. Low PiB PET retention in presence of pathologic CSF biomarkers in Arctic APP mutation carriers. Neurology. 2012;79:229-36.
[14] Bateman RJ, Xiong C, Benzinger TL, Fagan AM, Goate A, Fox NC, et al. Clinical and biomarker changes in dominantly inherited Alzheimer's disease. N Engl J Med. 2012;367:795-804.
[15] Fleisher AS, Chen K, Quiroz YT, Jakimovich LJ, Gomez MG, Langois CM, et al. Florbetapir PET analysis of amyloid-beta deposition in the presenilin 1 E280A autosomal dominant Alzheimer's disease kindred: a cross-sectional study. Lancet Neurol. 2012;11:1057-65.
[16] Tomiyama T, Nagata T, Shimada H, Teraoka R, Fukushima A, Kanemitsu H, et al. A new amyloid beta variant favoring oligomerization in Alzheimer's-type dementia. Ann Neurol. 2008;63:377-87.
[17] Bogdanovic N, Corder E, Lannfelt L, Winblad B. APOE polymorphism and clinical duration determine regional neuropathology in Swedish APP(670, 671) mutation carriers: implications for late-onset Alzheimer's disease. J Cell Mol Med. 2002;6:199-214.

[18] Ossenkoppele R, Jansen WJ, Rabinovici GD, Knol DL, van der Flier WM, van Berckel BN, et al. Prevalence of amyloid PET positivity in dementia syndromes: a meta-analysis. JAMA. 2015;313:1939-49.
[19] Scholl M, Carter SF, Westman E, Rodriguez-Vieitez E, Almkvist O, Thordardottir S, et al. Early astrocytosis in autosomal dominant Alzheimer's disease measured in vivo by multi-tracer positron emission tomography. Sci Rep. 2015;5:16404.
[20] Schmidt ME, Chiao P, Klein G, Matthews D, Thurfjell L, Cole PE, et al. The influence of biological and technical factors on quantitative analysis of amyloid PET: Points to consider and recommendations for controlling variability in longitudinal data. Alzheimers Dement. 2015;11:1050-68.
[21] Kepe V, Moghbel MC, Langstrom B, Zaidi H, Vinters HV, Huang SC, et al. Amyloid-beta positron emission tomography imaging probes: a critical review. J Alzheimers Dis. 2013;36:613-31.
[22] Cole GB, Keum G, Liu J, Small GW, Satyamurthy N, Kepe V, et al. Specific estrogen sulfotransferase (SULT1E1) substrates and molecular imaging probe candidates. Proc Natl Acad Sci U S A. 2010;107:6222-7.
[23] Forsberg A, Engler H, Almkvist O, Blomquist G, Hagman G, Wall A, et al. PET imaging of amyloid deposition in patients with mild cognitive impairment. Neurobiol Aging. 2008;29:1456-65.
[24] Villemagne VL, Mulligan RS, Pejoska S, Ong K, Jones G, O'Keefe G, et al. Comparison of 11C-PiB and 18F-florbetaben for Abeta imaging in ageing and Alzheimer's disease. Eur J Nucl Med Mol Imaging. 2012;39:983-9.
[25] Vandenberghe R, Van Laere K, Ivanoiu A, Salmon E, Bastin C, Triau E, et al. 18F-flutemetamol amyloid imaging in Alzheimer disease and mild cognitive impairment: A phase 2 trial. Annals of Neurology. 2010;68:319-29.
[26] Curtis C, Gamez JE, Singh U, Sadowsky CH, Villena T, Sabbagh MN, et al. Phase 3 trial of flutemetamol labeled with radioactive fluorine 18 imaging and neuritic plaque density. JAMA Neurol. 2015;72:287-94.
[27] Rowe CC, Pejoska S, Mulligan RS, Jones G, Chan JG, Svensson S, et al. Head-to-head comparison of 11C-PiB and 18F-AZD4694 (NAV4694) for beta-amyloid imaging in aging and dementia. J Nucl Med. 2013;54:880-6.
[28] Landau SM, Thomas BA, Thurfjell L, Schmidt M, Margolin R, Mintun M, et al. Amyloid PET imaging in Alzheimer's disease: a comparison of three radiotracers. Eur J Nucl Med Mol Imaging. 2014;41:1398-407.
[29] Parent M, Zimmer ER, Shin M, Kang M, DoCarmo S, Aliaga A, et al. Competitive binding of [11C]PIB AND [18F]NAV4694 in a transgenic rat model of amyloidosis. Alzheimer's & Dementia: The Journal of the Alzheimer's Association. 2014;10:P893.
[30] Kadir A, Marutle A, Gonzalez D, Scholl M, Almkvist O, Mousavi M, et al. Positron emission tomography imaging and clinical progression in relation to molecular pathology in the first Pittsburgh Compound B positron emission tomography patient with Alzheimer's disease. Brain. 2010;134:301-17.
[31] Niedowicz DM, Beckett TL, Matveev S, Weidner AM, Baig I, Kryscio RJ, et al. Pittsburgh compound B and the postmortem diagnosis of Alzheimer disease. Ann Neurol. 2012;72:564-70.
[32] Lockhart A, Lamb JR, Osredkar T, Sue LI, Joyce JN, Ye L, et al. PIB is a non-specific imaging marker of amyloid-beta (Abeta) peptide-related cerebral amyloidosis. Brain. 2007;130:2607-15.
[33] Clark CM, Pontecorvo MJ, Beach TG, Bedell BJ, Coleman RE, Doraiswamy PM, et al. Cerebral PET with florbetapir compared with neuropathology at autopsy for detection of neuritic amyloid-beta plaques: a prospective cohort study. Lancet Neurol. 2012;11:669-78.
[34] Matveev SV, Spielmann HP, Metts BM, Chen J, Onono F, Zhu H, et al. A distinct subfraction of Abeta is responsible for the high-affinity Pittsburgh compound B-binding site in Alzheimer's disease brain. J Neurochem. 2014;131:356-68.

[35] Kung HF, Choi SR, Qu W, Zhang W, Skovronsky D. 18F stilbenes and styrylpyridines for PET imaging of A beta plaques in Alzheimer's disease: a miniperspective. J Med Chem. 2010;53:933-41.
[36] Neumaier B, Deisenhofer S, Furst D, von Arnim CA, Thees S, Buck AK, et al. Radiosynthesis and evaluation of [11C]BTA-1 and [11C]3'-Me-BTA-1 as potential radiotracers for in vivo imaging of beta-amyloid plaques. Nuklearmedizin. 2007;46:271-80.
[37] Forsberg A, Jureus A, Cselenyi Z, Eriksdotter M, Freund-Levi Y, Jeppsson F, et al. Low background and high contrast PET imaging of amyloid-beta with [11C]AZD2995 and [11C]AZD2184 in Alzheimer's disease patients. Eur J Nucl Med Mol Imaging. 2013;40:580-93.
[38] Porat Y, Abramowitz A, Gazit E. Inhibition of amyloid fibril formation by polyphenols: structural similarity and aromatic interactions as a common inhibition mechanism. Chem Biol Drug Des. 2006;67:27-37.
[39] Ladiwala AR, Lin JC, Bale SS, Marcelino-Cruz AM, Bhattacharya M, Dordick JS, et al. Resveratrol selectively remodels soluble oligomers and fibrils of amyloid Abeta into off-pathway conformers. J Biol Chem. 2010;285:24228-37.
[40] Ahn JS, Lee JH, Kim JH, Paik SR. Novel method for quantitative determination of amyloid fibrils of alpha-synuclein and amyloid beta/A4 protein by using resveratrol. Anal Biochem. 2007;367:259-65.
[41] La Joie R, Perrotin A, Barre L, Hommet C, Mezenge F, Ibazizene M, et al. Region-Specific Hierarchy between Atrophy, Hypometabolism, and beta-Amyloid (Abeta) Load in Alzheimer's Disease Dementia. J Neurosci. 2012;32:16265-73.
[42] Lee I, Choe YS, Choi JY, Lee KH, Kim BT. Synthesis and evaluation of (1)(8)F-labeled styryltriazole and resveratrol derivatives for beta-amyloid plaque imaging. J Med Chem. 2012;55:883-92.
[43] Witte AV, Kerti L, Margulies DS, Floel A. Effects of resveratrol on memory performance, hippocampal functional connectivity, and glucose metabolism in healthy older adults. J Neurosci. 2014;34:7862-70.
[44] Cairns NJ, Perrin RJ, Franklin EE, Carter D, Vincent B, Xie M, et al. Neuropathologic assessment of participants in two multi-center longitudinal observational studies: the Alzheimer Disease Neuroimaging Initiative (ADNI) and the Dominantly Inherited Alzheimer Network (DIAN). Neuropathology. 2015;35:390-400.
[45] Haltia M, Viitanen M, Sulkava R, Ala-Hurula V, Poyhonen M, Goldfarb L, et al. Chromosome 14-encoded Alzheimer's disease: genetic and clinicopathological description. Ann Neurol. 1994;36:362-7.
[46] Lannfelt L, Bogdanovic N, Appelgren H, Axelman K, Lilius L, Hansson G, et al. Amyloid precursor protein mutation causes Alzheimer's disease in a Swedish family. Neurosci Lett. 1994;168:254-6.
[47] Houlden H, Baker M, McGowan E, Lewis P, Hutton M, Crook R, et al. Variant Alzheimer's disease with spastic paraparesis and cotton wool plaques is caused by PS-1 mutations that lead to exceptionally high amyloid-beta concentrations. Ann Neurol. 2000;48:806-8.
[48] Verkkoniemi A, Kalimo H, Paetau A, Somer M, Iwatsubo T, Hardy J, et al. Variant Alzheimer disease with spastic paraparesis: neuropathological phenotype. J Neuropathol Exp Neurol. 2001;60:483-92.
[49] Crook R, Verkkoniemi A, Perez-Tur J, Mehta N, Baker M, Houlden H, et al. A variant of Alzheimer's disease with spastic paraparesis and unusual plaques due to deletion of exon 9 of presenilin 1. Nat Med. 1998;4:452-5.
[50] Lu JX, Qiang W, Yau WM, Schwieters CD, Meredith SC, Tycko R. Molecular structure of beta-amyloid fibrils in Alzheimer's disease brain tissue. Cell. 2013;154:1257-68.

Table 1

Demographic information for sporadic and autosomal dominant Alzheimer's disease cases

Cohort	N	Age (range)	Sex (F/M)	*APOE* ε4 (0/1/2)	Disease duration (y)	Postmortem delay (h)
sAD	13	68.9 ± 8.5 (58–81)	7/6	3/3/7	6.1 ± 3.2	5.0 ± 0.9
ADAD	6	57.8 ± 10.6 (43–68)	3/3	4/1/1	9.5 ± 4.0	19.6 ± 8.7
APPswe	3	56–68	0/3	2/0/1	9.3 ± 2.2	21.7 ± 1.3
PS1 M146V	2	43–48	2/0	1/1/0	4–10	28
PS1 EΔ9	1	66	1/0	1/0/0	14	5
Ctrl	14	74.1 ± 12.0 (50–88)	5/9	14/0/0	—	7.3 ± 3.8

Abbreviations: sAD, sporadic Alzheimer's disease; ADAD, autosomal dominant Alzheimer's disease; *APPswe*, Swedish *APP* mutation carrier; *PS1 M146V*, *Presenilin 1 M146V* mutation carrier; *PS1 EΔ9*, *Presenilin 1* exon 9 deletion; Ctrl, healthy age-matched controls; *APOE*, apolipoprotein E; 0/1/2, number of ε4 allele.

NOTE. Data are shown as mean ± standard deviation (SD).

Table 2

Regional distribution of amyloid tracer ^{3}H-PIB (1.0 nM) and ^{3}H-AZD2184 (1.5 nM) binding in brain from sporadic, autosomal dominant Alzheimer's disease and healthy controls

Brain region	Ligand	ADAD	sAD	Control
Frontal cortex	^{3}H-PIB (pmol/g tissue)	212.2 ± 46.5** (n = 5)	219.0 ± 66.6*** (n = 8)	15.4 ± 20.5 (n = 14)
	^{3}H-AZD2184 (pmol/g tissue)	409.9 ± 171.6** (n = 5)	273.4 ± 103.7*** (n = 8)	19.9 ± 31.0 (n = 14)
Striatum	^{3}H-PIB (pmol/g tissue)	133.7 ± 43.5*** (n = 6)	53.7 ± 68.9# (n = 7)	5.6 ± 8.3 (n = 8)
	^{3}H-AZD2184 (pmol/g tissue)	237.5 ± 85.2* (n = 6)	179.7 ± 172.6 (n = 7)	27.7 ± 32.6 (n = 6)

Abbreviations: sAD, sporadic Alzheimer's disease; ADAD, autosomal dominant Alzheimer's disease; ^{3}H-PIB, ^{3}H-Pittsburgh compound B.

NOTE. Data are presented as means ± standard deviation (SD).

NOTE. Significant differences compared to control group (Mann–Whitney *U* test) are indicated by **P* < .05, ***P* < .01, ****P* < .001. Significant difference between ADAD and sAD group is indicated by #*P* < .05.

Fig. 1

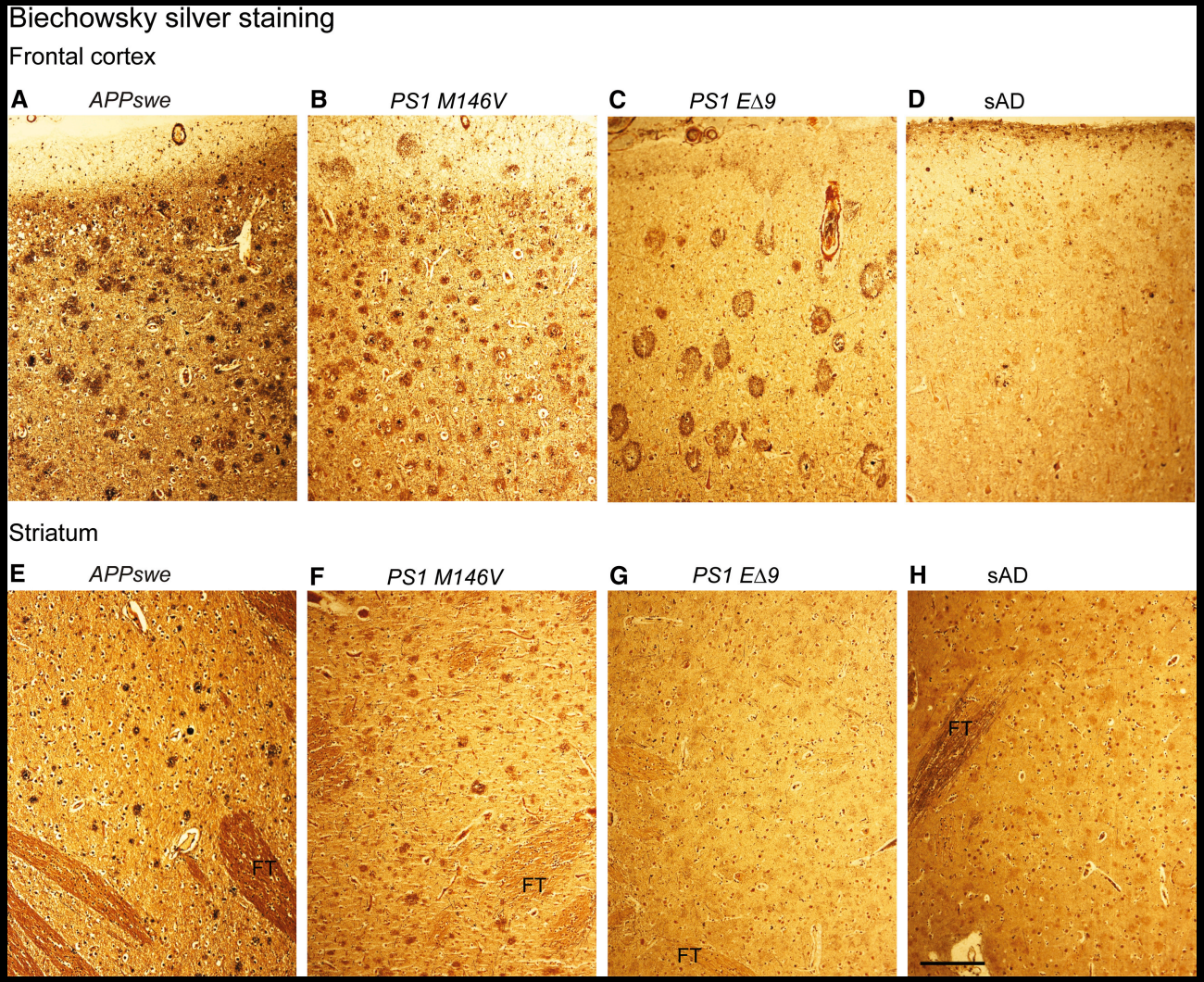

Alzheimer's & Dementia: The Journal of the Alzheimer's Association DOI: (10.1016/j.jalz.2016.08.006)

Fig. 2

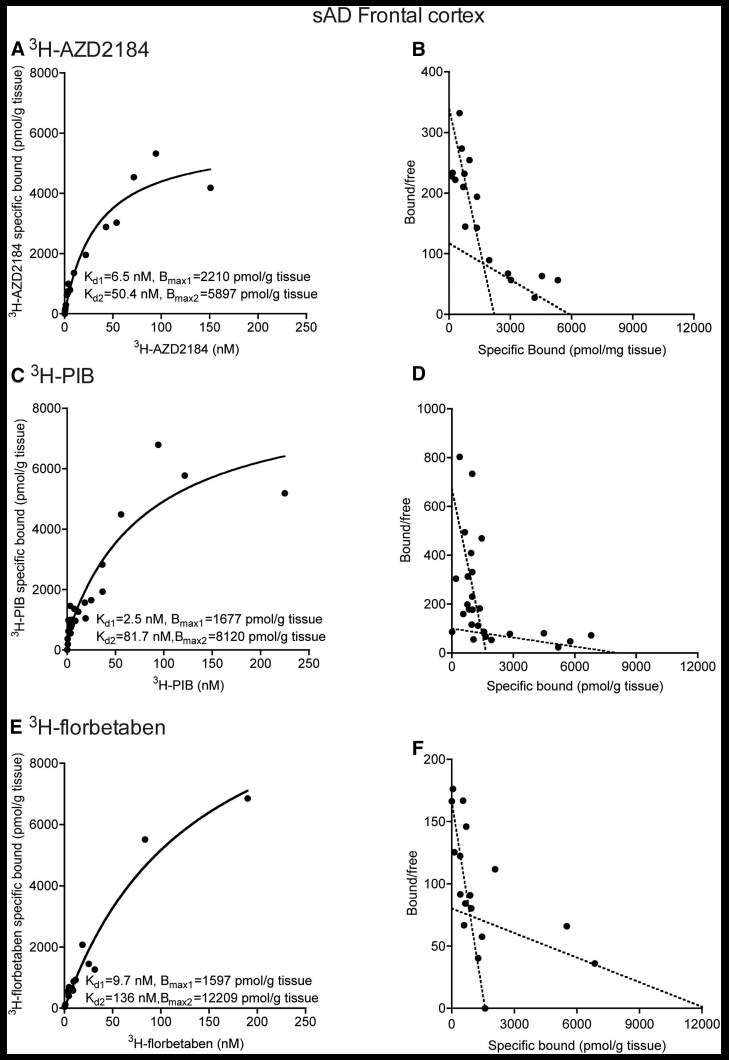

Alzheimer's & Dementia: The Journal of the Alzheimer's Association DOI: (10.1016/j.jalz.2016.08.006)

Fig. 3

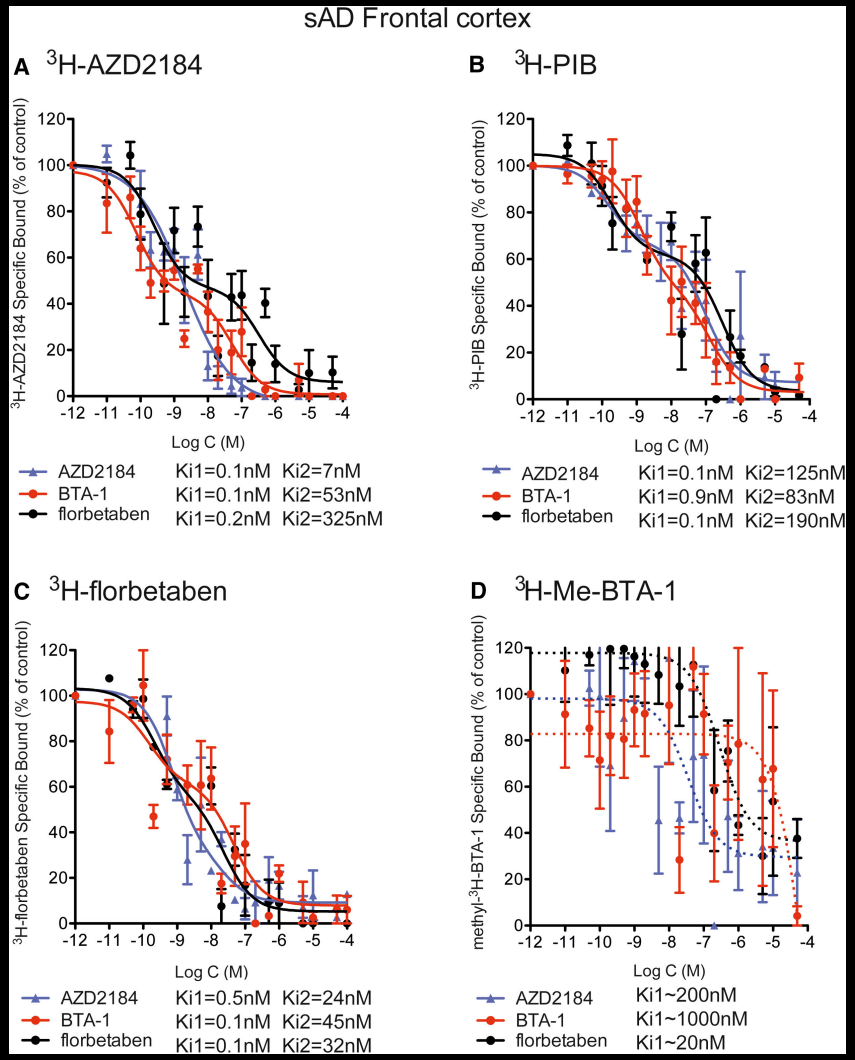

Alzheimer's & Dementia: The Journal of the Alzheimer's Association DOI: (10.1016/j.jalz.2016.08.006)

Fig. 4

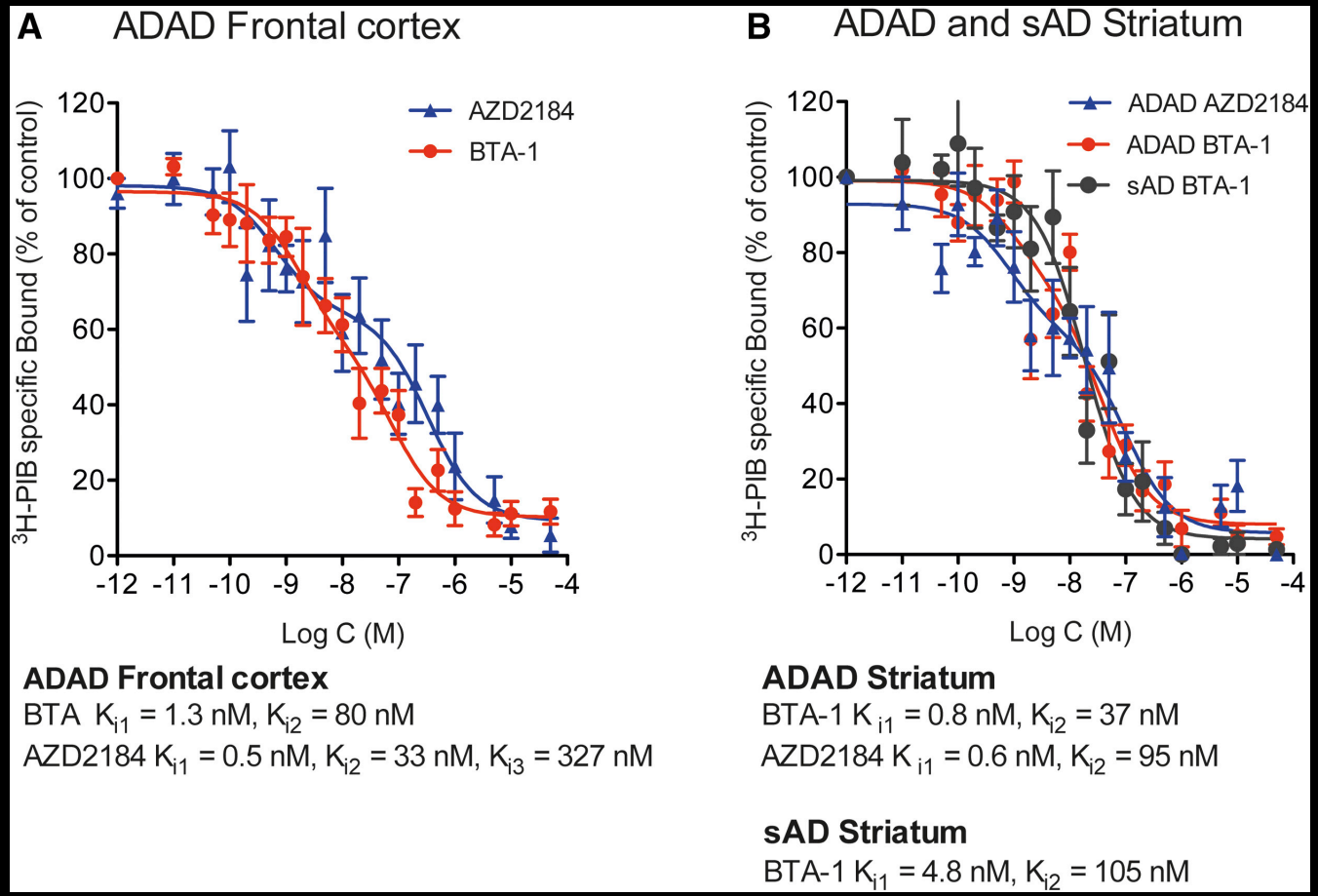

Alzheimer's & Dementia: The Journal of the Alzheimer's Association DOI: (10.1016/j.jalz.2016.08.006)

Fig. 5

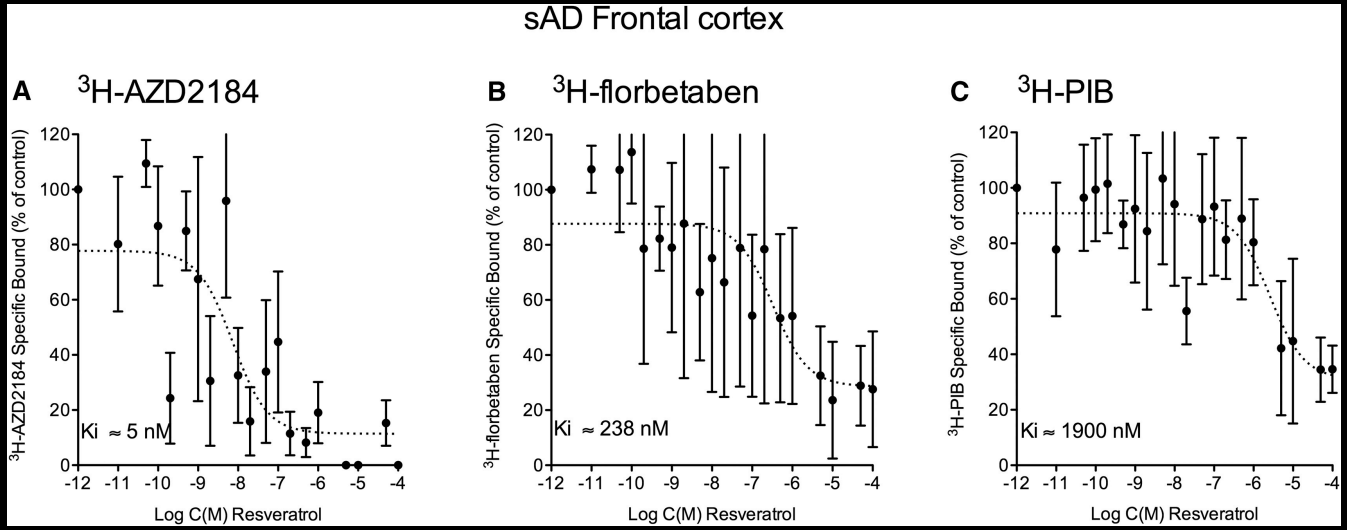

Alzheimer's & Dementia: The Journal of the Alzheimer's Association DOI: (10.1016/j.jalz.2016.08.006)

Fig. 6

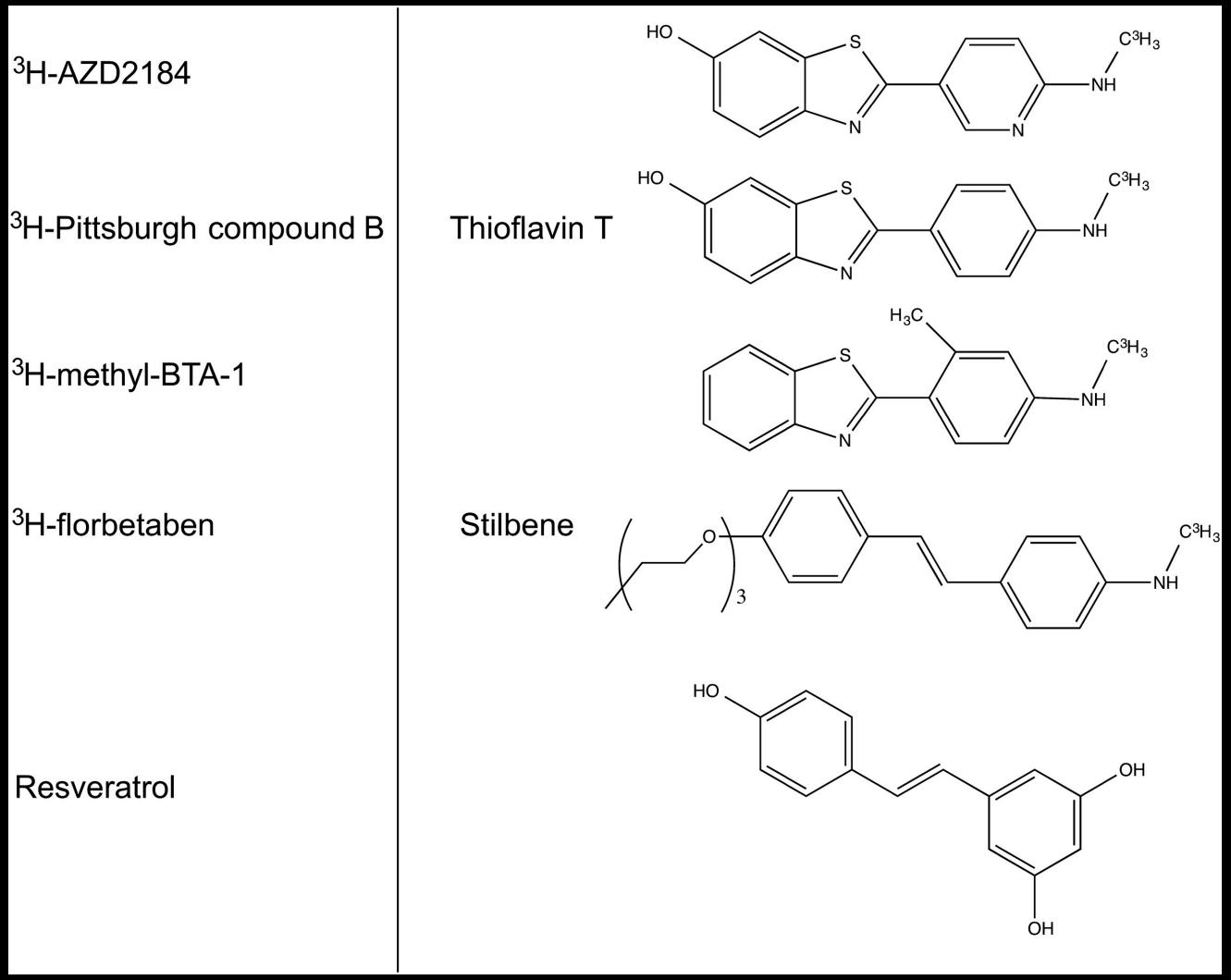

Alzheimer's & Dementia: The Journal of the Alzheimer's Association DOI: (10.1016/j.jalz.2016.08.006)